

Supporting Information

Extending the Propagation Distance of a Silver Nanowire Plasmonic Waveguide with a Dielectric Multilayer Substrate

Douguo Zhang^{1*}, Yifeng Xiang¹, Junxue Chen^{2*}, Junjie Cheng³, Liangfu Zhu¹, Ruxue Wang¹, Gang Zou³, Pei Wang¹, Hai Ming¹, Mary Rosenfeld⁴, Ramachandram Badugu⁴, and Joseph R. Lakowicz⁴

¹Institute of Photonics, Department of Optics and Optical Engineering, University of Science and Technology of China, Hefei, Anhui, 230026, P.R. China

²School of Science, Southwest University of Science and Technology, Mianyang, Sichuan 621010, P.R. China

³CAS Key Laboratory of Soft Matter Chemistry, Department of Polymer Science and Engineering, iChEM, University of Science and Technology of China, Hefei, Anhui 230026, P.R. China

⁴Center for Fluorescence Spectroscopy, Department of Biochemistry and Molecular Biology, University of Maryland School of Medicine, Baltimore, MD 21201, United States

Correspondence and requests for materials should be addressed to D.G. Zhang (Email: dgzhang@ustc.edu.cn)

or J. X. Chen (Email: cjxueoptics@163.com).

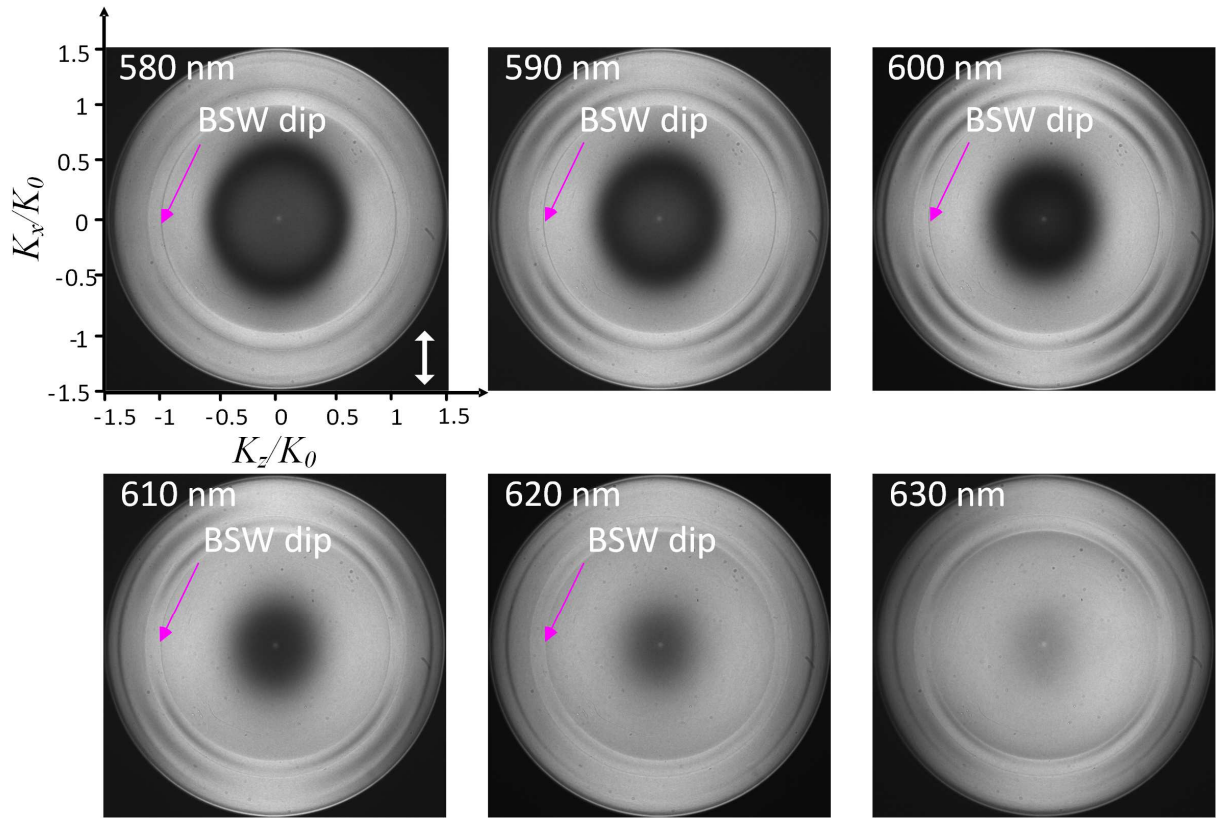


Figure S1 | BFP images of white light reflected from the dielectric multilayer. An expanded white light beam was used to fill the rear aperture of the oil-immersed objective (100 \times and N.A. of 1.49). The reflected beam at the BFP of the objective was imaged onto a camera's detector. A series of band pass filters were placed before the camera to select the wavelength from the white light source. The centre wavelengths of the filters ranged from 580 to 630 nm. The dark dips between 580 and 620 nm, labelled as BSW dips, represent the excitation of the BSW mode at these wavelengths; those dips are equivalent to the dip in the angle-resolved total internal reflected curve measured with a prism setup. A 2DBSW was not excited on this multilayer for a wavelength of 630 nm or longer. There are other rings appear on the BFP image with larger diameter than that of BSW, which are attributed to the internal modes of the dielectric multilayer.

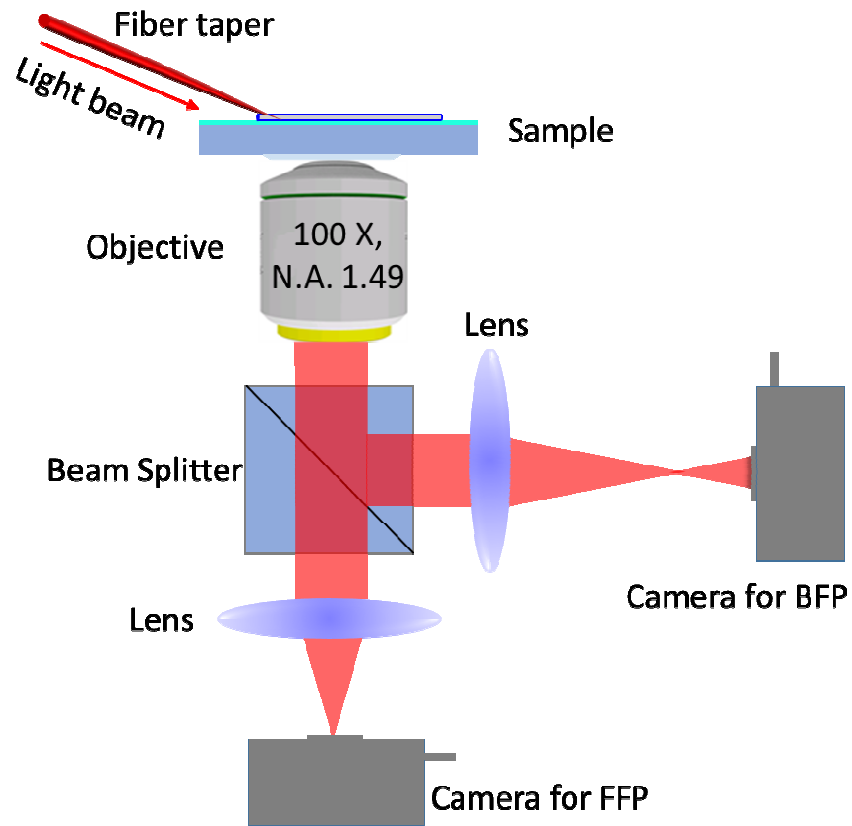


Figure S2| Schematic of the experimental set-up for imaging the Plasmonic signals propagating along the silver nanowire. Two cameras are used for capturing the FFP and BFP images.

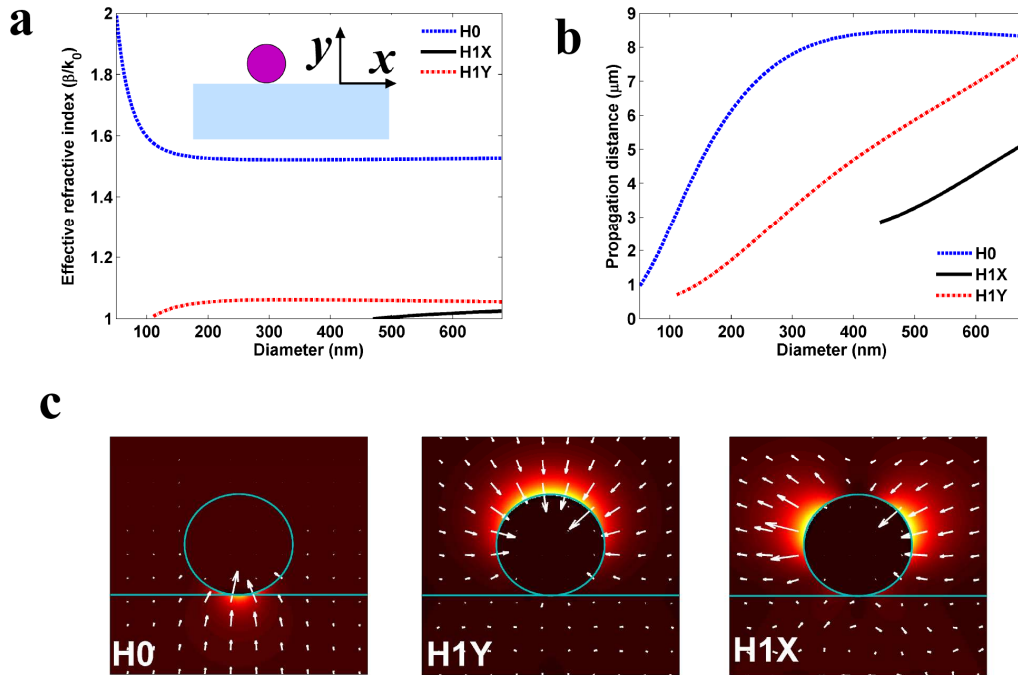


Figure S3| Diameter-dependent dispersion relation of plasmonic modes of a nanowire on the glass substrate. (a) The graph shows plots of the effective refractive index of plasmonic modes as a function of the nanowire diameter. There are three modes (H0, H1X, and H1Y) existing for a silver nanowire placed on a glass substrate (inset graph in (a)). (b) The propagation distance of the three plasmonic modes versus the nanowire diameter. (c) The electric field distributions for H0, H1Y and H1X modes with diameter of a silver nanowire at 500 nm. The incident wavelength is fixed at 630 nm. The white arrows in panels (c) denote vectors showing the direction of the electric field.

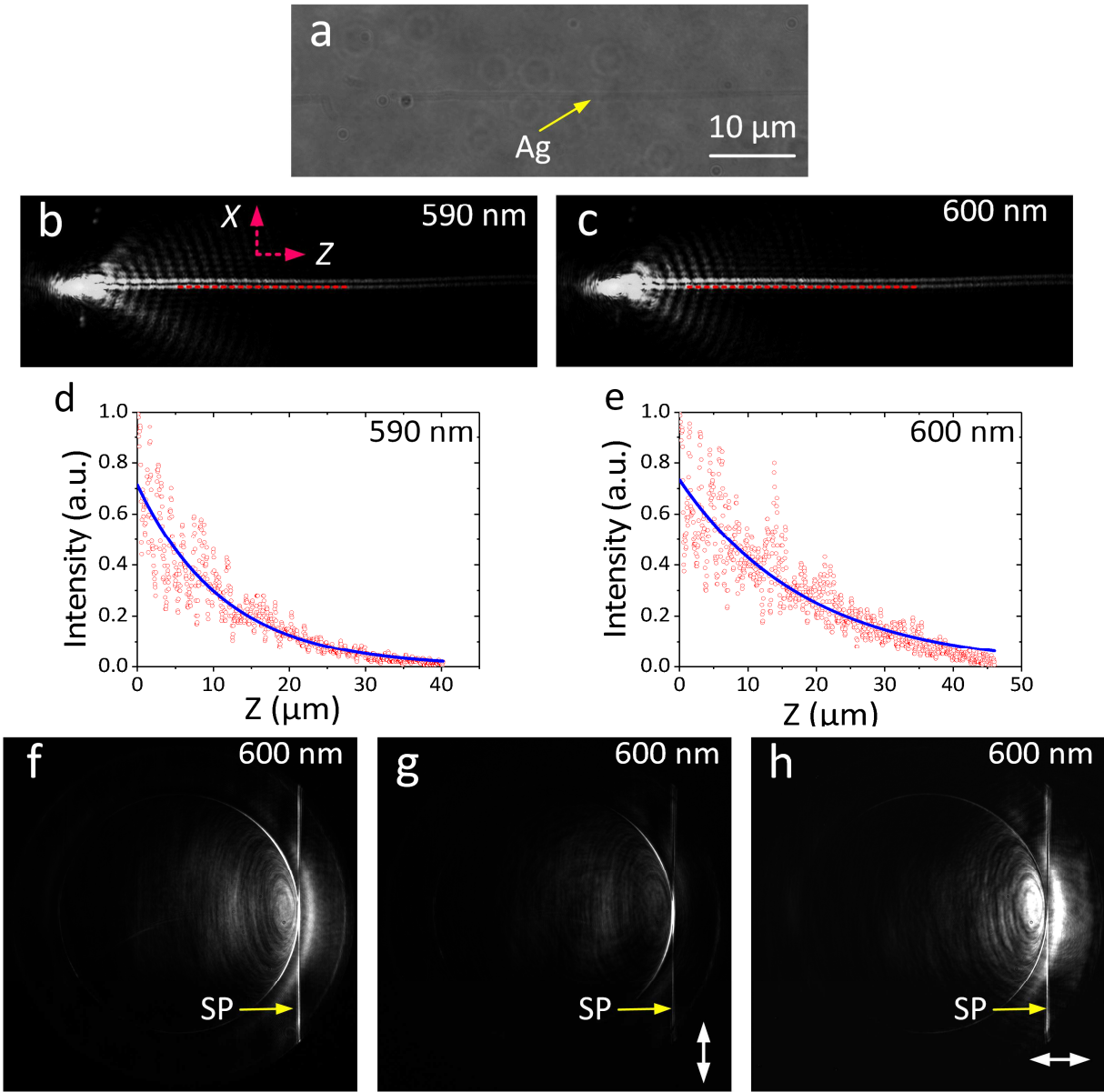


Figure S4| Propagation distance and polarization states of the plasmonic leaky mode with the diameter of the silver nanowire at 70 nm. (a) White light image of the 70 nm diameter silver nanowire on the multilayer. The location of the Ag is the darker line. FFP images of the laser beam propagating along the silver nanowire for an incident wavelength at (b) 590 nm and (c) 600 nm. The intensity distribution along the nanowire (Z-direction, red dashed lines) in panels (b) and (c) are shown in panels (d) and (e), respectively. The blue solid line is an exponential fit to the data (red

dots) and was used to extract the propagation distance of the plasmonic leaky mode as 12 μm (at 590 nm) and 18 μm (at 600 nm). The scale bar in panel (a) is also applicable for panel (b, c). Panels (f) (g) and (h) show the corresponding BFP images with incident wavelength at 600 nm and a polarizer placed before the detector. The white double arrowhead lines represent the direction of the polarizer.

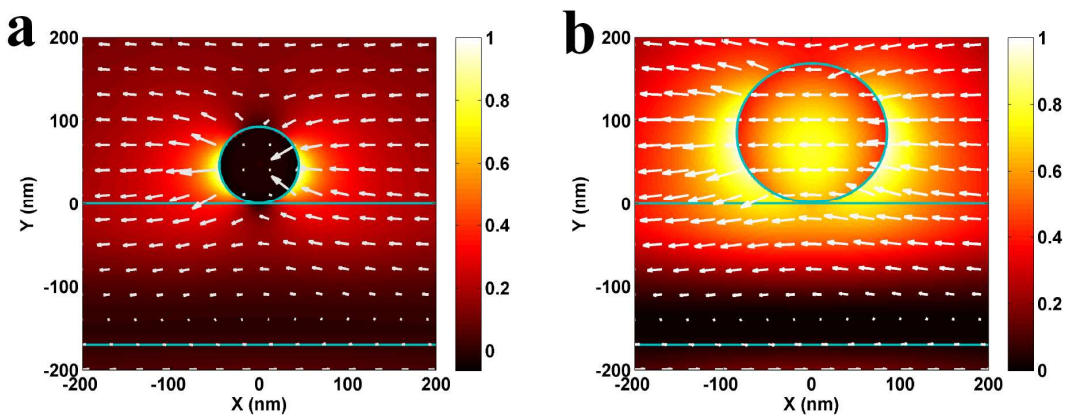


Figure S5| Electric field distributions of the plasmonic leaky mode (H1X mode) of an Ag nanowire and the one-dimensional BSW (BSW-1D) mode of a polymer nanowire. The two nanowires are placed on the same dielectric multilayer. (a) The electric field distribution of the leaky mode of an Ag nanowire placed on the dielectric multilayer. (b) The electric field distribution of the BSW-1D mode of a nanowire placed on the dielectric multilayer. Here, the diameter of the Ag nanowire and polymer nanowire were 90 and 170 nm, respectively. The wavelength was fixed at 630 nm. The white arrows in panels (a) and (b) denote vectors showing the direction of the electric field.

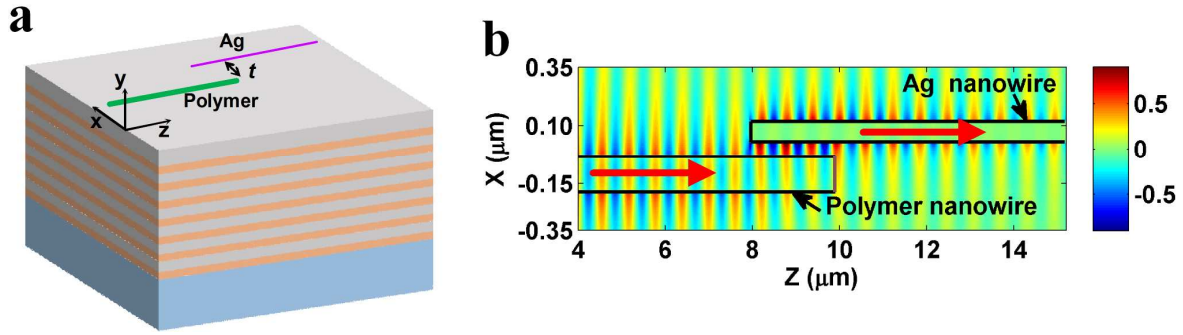


Figure S6| Coupling of the plasmonic leaky mode of a silver nanowire and the BSW-1D mode of a polymer nanowire. (a) Schematic illustration of the coupled nanowire in our simulation. The separation between the two nanowires is denoted as t . (b) The distribution of the electric field E_x of the coupled nanowires with a separation of $t = 60$ nm. The fields were obtained at 45 nm above the surface of the dielectric multilayer. The diameters of the silver and polymer nanowires were 90 and 170 nm, respectively. The incident wavelength was 630 nm. The red arrows denote the propagation direction of the surface waves along each nanowire.

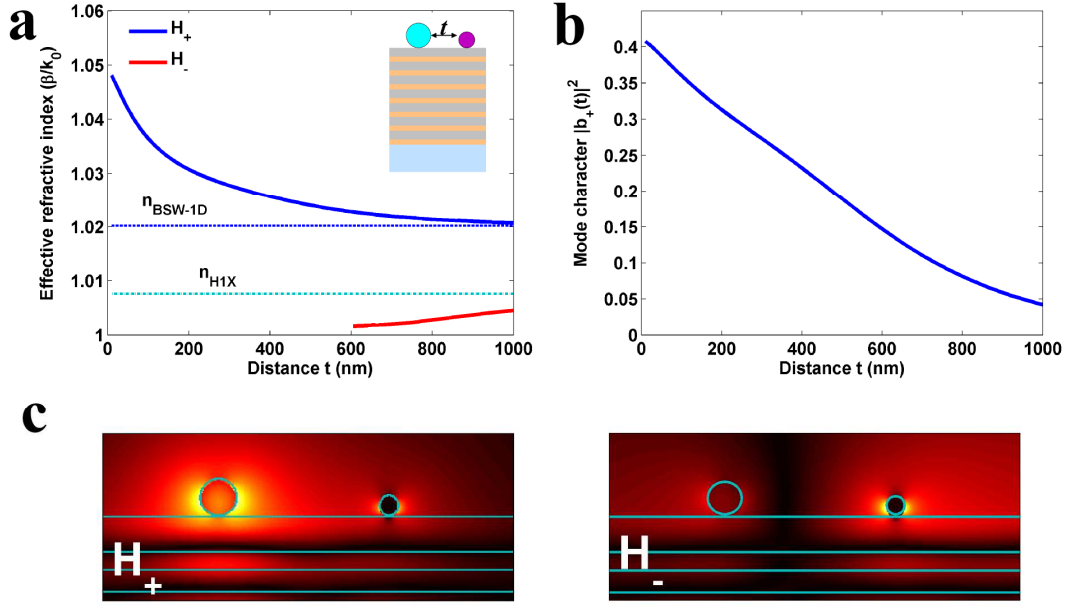


Figure S7| Distance-dependent dispersion relation of the coupled modes. The H1X mode of a Ag nanowire can be coupled with the BSW-1D mode of a polymer nanowire to form the in-phase coupled mode (H_+) and out-of phase coupled mode (H_-). (a) the effective refractive index of the coupled modes H_+ and H_- as a function of the separation distance t . (b) the coupling coefficient between H1X mode and BSW-1D mode versus the separation distance t . The electric field distributions for H_+ and H_- modes with separation $t = 700$ nm are calculated as shown in (c) and (d), respectively. The diameters of the silver and polymer nanowires were 90 and 170 nm, respectively. The incident wavelength was 630 nm.

We can describe the coupled modes as a linear superposition of the BSW-1D mode (without the Ag nanowire) and the H1X mode (without the polymer nanowire) according to the coupled mode theory [26].

$$\psi_{\pm}(t) = a_{\pm}(t)\psi_{BSW-1D} + b_{\pm}(t)\psi_{H1X} \quad (S1)$$

Where $a_{\pm}(t)$ and $b_{\pm}(t) = \sqrt{1 - |a_{\pm}(t)|^2}$ are the amplitudes of the BSW-1D mode and H1X mode, respectively. The signs + and - are corresponding to the in-phase and out-of-phase coupled modes,

respectively. The square norm of the H1X mode amplitude $|b_+(t)|^2$ provides a measure of the hybridization strength of the coupled modes. The modes of the coupled system can be described by a two-dimensional matrix.

$$\begin{pmatrix} n_{BSW-1D}(t) & V(t) \\ V(t) & n_{H1X}(t) \end{pmatrix} \begin{pmatrix} a_{\pm}(t) \\ b_{\pm}(t) \end{pmatrix} = n_{\pm}(t) \begin{pmatrix} a_{\pm}(t) \\ b_{\pm}(t) \end{pmatrix} \quad (S2)$$

where $V(t)$ is the coupling strength between BSW-1D and H1X modes. n_{BSW-1D} and n_{H1X} are the effective refractive index of the BSW-1D and H1X modes, respectively. The solutions of the Eq.(S2) are given by

$$n_+(t) = \frac{n_{BSW-1D} + n_{H1X} + \sqrt{(n_{BSW-1D} - n_{H1X})^2 + 4V^2}}{2} \quad (S3)$$

$$n_-(t) = \frac{n_{BSW-1D} + n_{H1X} - \sqrt{(n_{BSW-1D} - n_{H1X})^2 + 4V^2}}{2} \quad (S4)$$

Then, the mode amplitude $|b_+(t)|^2$ can be expressed as

$$|b_+(t)|^2 = \frac{(n_+ - n_{BSW-1D})^2}{(n_+ - n_{BSW-1D})^2 + V^2} \quad (S5)$$